Biol. Chem., Vol. 386, pp. 1129–1136, November 2005 • Copyright © by Walter de Gruyter • Berlin • New York. DOI 10.1515/BC.2005.129

Plasmodium falciparum 2-Cys peroxiredoxin reacts with plasmoredoxin and peroxynitrite

Christine Nickel[1], Madia Trujillo[2], Stefan Rahlfs[1], Marcel Deponte[1], Rafael Radi[2] and Katja Becker[1,*]

[1] Interdisciplinary Research Centre, Justus-Liebig-University, D-35392 Giessen, Germany
[2] Departamento de Bioquímica and Center for Free Radical and Biomedical Research, Facultad de Medicina, UY-11800 Montevideo, Uruguay

* Corresponding author
e-mail: becker.katja@gmx.de

Abstract

Thioredoxin peroxidase 1 (TPx1) of the malarial parasite *Plasmodium falciparum* is a 2-Cys peroxiredoxin involved in the detoxification of reactive oxygen species and – as shown here – of reactive nitrogen species. As novel electron acceptor of reduced TPx1, we characterised peroxynitrite; the rate constant for $ONOO^-$ reduction by the enzyme (1×10^6 M^{-1} s^{-1} at pH 7.4 and 37°C) was determined by stopped-flow measurements. As reducing substrate of TPx1, we identified – aside from thioredoxin – plasmoredoxin; this 22-kDa protein occurs only in malarial parasites. When studying the potential roles of Cys74 and Cys170 of Tpx1 in catalysis, as well as in oligomerisation behaviour, we found that replacement of Cys74 by Ala influenced neither the dimerisation nor enzymatic activity of TPx1. In the C170A mutant, however, the k_{cat}/K_m for reduced Trx as a substrate was shown to be approximately 50-fold lower and, in contrast to the wild-type enzyme, covalently linked dimers were not formed. For the catalytic cycle of TPx1, we conclude that oxidation of the peroxidatic Cys50 by the oxidising substrate is followed by the formation of an intermolecular disulfide bond between Cys50 and Cys170′ of the second subunit, which is then attacked by an external electron donor such as thioredoxin or plasmoredoxin.

Keywords: antioxidant; malaria; peroxiredoxin; peroxynitrite; *Plasmodium*; plasmoredoxin; thioredoxin system.

Introduction

The redox metabolism of the malarial parasite *Plasmodium falciparum* represents a promising target for urgently required antimalarial drugs (Becker et al., 2004; Krauth-Siegel et al., 2005). Most interestingly, the parasite possesses neither a catalase nor a classical glutathione peroxidase, demonstrating that its antioxidant defence differs significantly from that of its human host. However, five different peroxidases have been described in *Plasmodium* so far. Two of these enzymes (TPx1 and TPx2) are 2-Cys peroxiredoxins (Prx). For TPx1, thioredoxin-dependent peroxidase activity (Krnajski et al., 2001; Rahlfs and Becker, 2001), as well as its involvement in the *in vivo* detoxification of peroxides (Akerman and Müller, 2003; Komaki-Yasuda et al., 2003), has been demonstrated. The protein oligomerises to $(\alpha_2)_5$ decamers and reacts very efficiently with H_2O_2 ($k_{cat}/K_m \approx 6.7\times10^6$ M^{-1} s^{-1} at 30°C; Akerman and Müller, 2003). The third Prx of malarial parasites belongs to the 1-Cys group. To date, the specificity for the reducing substrate of this enzyme remains unclear (Kawazu et al., 2000, 2005; Krnajski et al., 2001), as is the case for many 1-Cys Prxs of other organisms (Pedrajas et al., 2000; Deponte and Becker, 2005). The fourth peroxidase (TPx_{Gl}) is not a Prx, but shows high sequence similarity with glutathione peroxidases (GPx; Gamain et al., 1996), although it prefers reduced thioredoxin (Trx) as substrate (Sztajer et al., 2001). Very recently, a type-V Prx named antioxidant protein (AOP) was identified, and its crystal structure has been solved (Sarma et al., 2005).

Apart from a classical and highly active Trx, *P. falciparum* possesses a typical glutaredoxin (Grx), as well as a number of Trx- and Grx-like proteins (Rahlfs et al., 2002, 2003; Deponte et al., 2005). In addition, plasmoredoxin (Plrx), a 22-kDa redox-active protein that is highly conserved among malarial parasites, is likely to contribute to redox homeostasis (Becker et al., 2003). Plrx is unique to *Plasmodium* spp., comprises 179 amino acid residues (*P. falciparum*) with a WCKYC motif at the active site, and may be classified as a member of the thioredoxin superfamily. It has been shown that the protein is reduced *in vitro* by PfGrx1 and *Trypanosoma brucei brucei* tryparedoxin. Reduced Plrx was shown to reduce insulin and glutathione disulfide, as well as ribonucleotide reductase (Becker et al., 2003).

Peroxynitrite, a strong oxidant formed *in vivo* by the reaction between superoxide ($O_2^{\bullet-}$) and nitric oxide ($^{\bullet}NO$) (Estevez et al., 1999; Radi et al., 2000; Ischiropoulos, 2003), has been proposed as a principal effector molecule for macrophage-mediated cytotoxicity towards *P. falciparum* (Fritsche et al., 2001). Peroxynitrite permeates biological membranes and reacts directly with different targets, including carbon dioxide, thiols, and heme proteins (Radi et al., 1991b; Denicola et al., 1998; Trujillo and Radi, 2002). Various biomolecules are damaged by peroxynitrite through oxidation, nitration, and nitrosation reactions (Radi et al., 1991a; Douki et al., 1996; Quijano et al., 1997; Skinner et al., 1998; Arteel et al., 1999; Savvides et al., 2002). Peroxynitrite reacts (pK_a of peroxynitrous acid 6.8) with low-M_r thiols, including cysteine and glutathione, at moderate rates ($\sim10^3$ M^{-1} s^{-1} at pH 7.4 and 37°C) and at higher rates (10^5–10^8 M^{-1} s^{-1}) with a number of proteins, including glyceraldehyde-3-phosphate dehydrogenase (Souza and Radi, 1998), creatine kinase

Table 1 Oxidation of plasmoredoxin thiols by H_2O_2 in the presence of TPx1.

	s1	s2	s3	s4
Plasmoredoxin (10 μM)	+	+	+	+
PfTPx1 (8 μM)	–	+	+	–
H_2O_2 (20 μM)	–	+	–	+
SH-groups (μM) at t=10 s	38.8	26.0	39.0	39.2
SH-groups (μM) at t=15 min	38.6	19.5	37.6	26.3

The compositions of samples s1–s4 are given in the first three lines. Thiol groups were determined by addition of 400 μM DTNB (final concentration) after 10 s and 15 min, respectively. All values were corrected for controls carried out in the absence of Plrx. Plrx contains four SH-groups, two of which constitute the active site. The data represent two independent experiments, with values differing by less than 10%.

(Konorev et al., 1998), and bacterial alkyl hydroperoxide reductase C (AhpC) (Bryk et al., 2000).

PfTPx1 has been shown to protect parasite cells against reactive oxygen and nitrogen species (ROS and RNS, respectively) (Akerman and Müller, 2003; Komaki-Yasuda et al., 2003). To further enhance our understanding of the redox network in malarial parasites, we characterised plasmoredoxin and peroxynitrite as novel substrates of TPx1. Using site-directed mutagenesis and structural modelling, we also investigated the role of Cys74 and Cys170 in hydroperoxidase activity and oligomerisation behaviour.

Results

Plasmoredoxin as reducing substrate of TPx1

As shown in Table 1, prereduced Plrx was incubated with TPx1 and/or H_2O_2. The oxidation of SH groups was monitored with 5,5′-dithio-bis-(2-nitrobenzoic acid) (DTNB). Reduced Plrx possesses four SH groups per protein molecule, which is clearly reflected by the experimentally obtained value of 38.8 μM (sample 1). Plrx incubated with TPx1 in the absence of peroxide yielded an almost identical value of 39 μM thiol groups (3.9 SH groups per Plrx molecule, sample 3). In the absence of TPx1, Plrx does not instantaneously react with H_2O_2 (sample 4); however, after 15 min, oxidation of Plrx by H_2O_2 occurred, resulting in 26 μM residual thiol groups (2.6 SH groups per Plrx molecule). In the presence of TPx1 (sample 2), 13 μM thiol groups were consumed immediately (10 s) after the addition of peroxide. This demonstrates an electron transfer from Plrx via TPx1 to H_2O_2. After 15 min, a total loss of 19.5 μM SH groups (2.0 SH groups per molecule, 50% of the total SH groups) was measured, which is likely to represent the two active site thiols of Plrx.

Peroxynitrite as oxidising substrate of TPx1

To determine the second-order rate constant for the reaction between peroxynitrite and TPx1, an initial rate approach was used, mixing reduced TPx1 in 100 mM sodium phosphate buffer, pH 7.0, with 0.1 mM diethylenetriamine pentaacetic acid (DTPA) and peroxynitrite (20 μM) in dilute sodium hydroxide at a pH of 7.4 and 37°C. As shown in Figure 1A, TPx1 significantly accelerates the decomposition of peroxynitrite, with 50% of peroxynitrite consumed by TPx1 within 10 ms. From the slope of the plot of the initial rate of peroxynitrite decomposition at different enzyme concentrations (Figure 1A), divided by the concentration of peroxynitrite used in the assay, a second-order rate constant of 1×10^6 M^{-1} s^{-1} at pH 7.4 and 37°C was determined. In agreement with this, a second-order rate constant for the reaction of 4×10^5 M^{-1} s^{-1} was obtained at pH 7.4 and 25°C (data not shown).

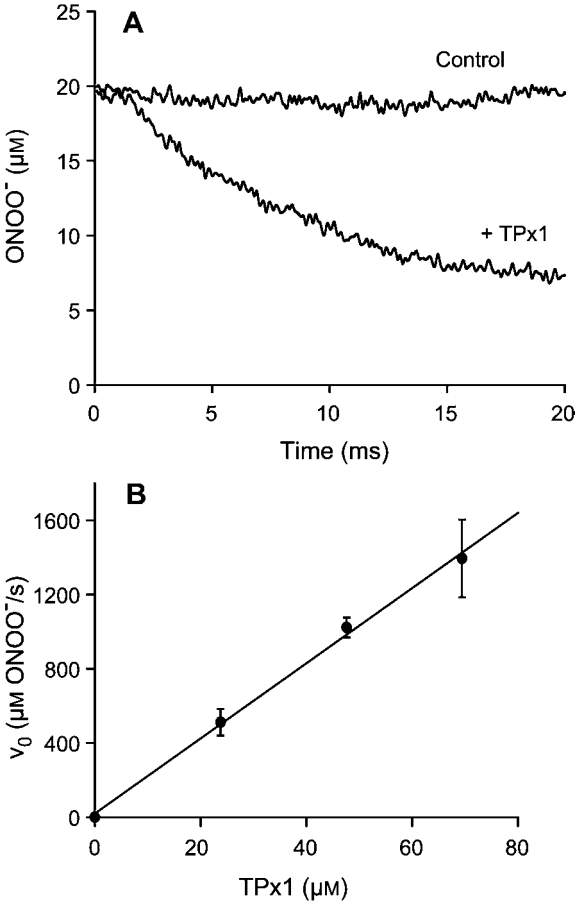

Figure 1 Peroxynitrite decomposition in the presence of reduced PfTPx1.
(A) Peroxynitrite (20 μM) decomposition in 50 mM sodium phosphate buffer, 0.1 mM DTPA at pH 7.4 and 37°C in the absence (control) or presence of reduced TPx1 (48 μM) was followed at 302 nm. (B) Initial rates of peroxynitrite decomposition under the same conditions as in (A) plotted against TPx1 concentration.

Impact of Cys74 and Cys170 on the activity and oligomerisation of TPx1

The role of the peroxidatic cysteine (approx. position 50 of most Prxs) has been studied for many other organisms (Hofmann et al., 2002; Deponte et al., 2005). To elucidate the function of the cysteine residues C74 and C170 of TPx1 for Trx-dependent activity, we generated alanine mutants and investigated their kinetic characteristics and oligomerisation behaviour compared to the wild type. As TPx1 is unstable in the presence of oxidising substrates (or just by exposure to air over time), all proteins were prepared freshly and under reducing conditions before use.

Table 2 Kinetic properties (thioredoxin-dependent H_2O_2 reducing activity) and covalent dimerisation of wild-type PfTPx1 and two mutants.

	Apparent K_m (μM)	Apparent V_{max} (U/mg)	Covalent dimerisation
PfTPx WT	23±1.3	1.9±0.3	Yes
PfTPx C74A	25±2.7	1.6±0.3	Yes
PfTPx C170A	40–190*	≤0.3	No

*The K_m value varied between different enzyme preparations. Due to the low specific activity of the mutant, rather high micromolar enzyme concentrations had to be used.

Trx-dependent peroxidase activity differed significantly among the enzyme species. Parameters obtained with TPx1C74A were similar to those of the wild type (Table 2). TPx1C170A, however, showed a higher apparent K_m (up to 190 μM, depending on the enzyme preparation) in comparison to the wild type (23 μM), suggesting decreased affinity for Trx. As the maximal activity deviated from the wild type by a factor of approximately six, the k_{cat}/K_m values were up to 50-fold lower for the C170A mutant. TPx1C170A was prone to precipitation during the purification process and storage; this could transiently be prevented by the addition of dithiothreitol in millimolar concentrations.

SDS-PAGE analysis of the three proteins under reducing and non-reducing conditions clearly indicated that – in contrast to C74A and wild-type enzyme – the TPx1 mutant C170A is not able to form a disulfide-linked dimer (Figure 2). The absence of decamers in the gel is due to the denaturing conditions used.

Molecular modelling of TPx1

The amino acid sequence of TPx1 shows 47% identity to human PrxII (Schröder et al., 2000) and 46% identity to rat PrxI (Hirotsu et al., 1999). Models of dimeric PfTPx1 with or without an intermolecular disulfide bond between Cys50 and Cys170′ were generated using the corresponding crystal structures of PrxI or PrxII. Tertiary and quaternary structure, as well as the calculated force field energies, of the models of TPx1 are similar to the templates (Figure 3I). In comparison to PrxI or PrxII, the loop between helix α1 and strand β3 of TPx1 is extended by one residue, and the loop between helix α4 and strand β6 is shortened by one amino acid. In addition, the loop after strand β1 of PrxII is shortened by one residue (for comparison of secondary structure, see Figure 1 of Hirotsu et al., 1999). According to the models generated, Cys50 and Cys170 of TPx1 are orthologues of the peroxidatic and resolving cysteine residues of mammalian typical 2-Cys Prx. In contrast to the N-terminally located residues Cys70 or Cys71 of PrxII or PrxI, respectively, Cys74 of TPx1 is located C-terminally on the strand β4. Thus, Cys74 is structurally different. Cys74 is hardly accessible in the models of PfTPx1. The Sγ-Sγ distance between Cys74 and Cys50 of reduced TPx1 is 10–13 Å, depending on the rotamers chosen. Cys50 of reduced TPx1 is located in the buried active-site pocket at the N-terminus of helix α2 (Figure 3IA). According to the model of TPx1, the N-terminus of helix α2 can be unwound, allowing the formation of a disulfide bond between Cys50 and Cys170′ of the second subunit (Figure 3IC). In the reduced state, Cys50 is located near Arg125 and Thr47, forming the classical active site of Prx (Hofmann et al., 2002).

Based on the crystal structure of human PrxII, a model of $(\alpha_2)_5$ decameric TPx1 was generated (Figure 3II). Recently, these (dimers of) doughnut-like structures of TPx1 have been detected by gel filtration and electron microscopy (Akerman and Müller, 2003). Interestingly, in TPx1 and PrxII, all but four residues of the dimer-dimer interface region II (Wood et al., 2003) – which comprises Ser75–Pro89, including Thr88, in TPx1 – are identical. In mammalian 2-Cys Prx, this region was shown to be involved in oligomerisation; here the conserved threonine residue is a target for phosphorylation, probably triggering the decomposition and/or enzymatic activity of the decamers (Wood et al., 2003). In contrast to PrxII, three neutral amino acids are replaced in TPx1 by Lys79, Lys86, and Lys87, with all of them being located on one side of helix α3.

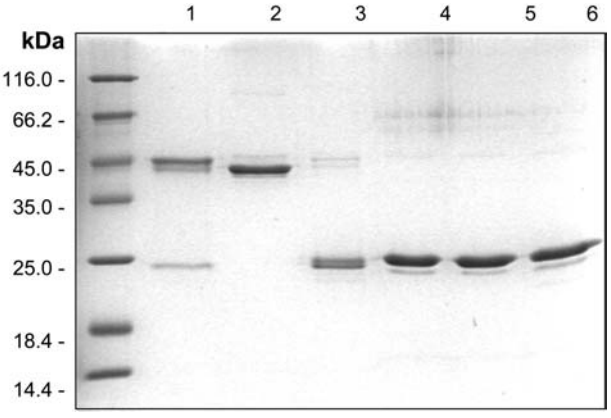

Figure 2 Analysis of purified recombinant proteins by SDS-PAGE.
Wild-type and mutants of PfTPx1 (2 μg/lane) were analysed by 15% SDS-PAGE without (lanes 1–3) and with (lanes 4–6) 1 mM dithiothreitol as reductant. Lanes 1 and 4, wild type; lanes 2 and 5, C74A; lanes 3 and 6, C170A.

Discussion

The intracellular interdependence of the thioredoxin and glutathione systems in malarial parasites has been suggested by Kanzok et al. (2000, 2001), who demonstrated that glutathione disulfide can be reduced by Trx. As shown here, this interdependence is further supported by the fact that TPx1 accepts electrons from plasmoredoxin. Plrx itself can be reduced by PfGrx1 and, with lower efficiency, by Trx1, dihydrolipoamide and glutathione. Plrx was shown to reduce ribonucleotide reductase (Becker et al., 2003) and, as demonstrated here (Table 1, sample 4), it is also able to directly degrade H_2O_2. So far, there is no enzyme assay to spectrophotometrically monitor the catalytic oxidation of Plrx by hydroperoxides in the presence of TPx1. However, our data clearly show that the electron transfer from Plrx to H_2O_2 in the presence of TPx1 (Table 1, sample 2) is much faster than the direct reduction of H_2O_2 by Plrx (Table 1, sample 4). Thus, the

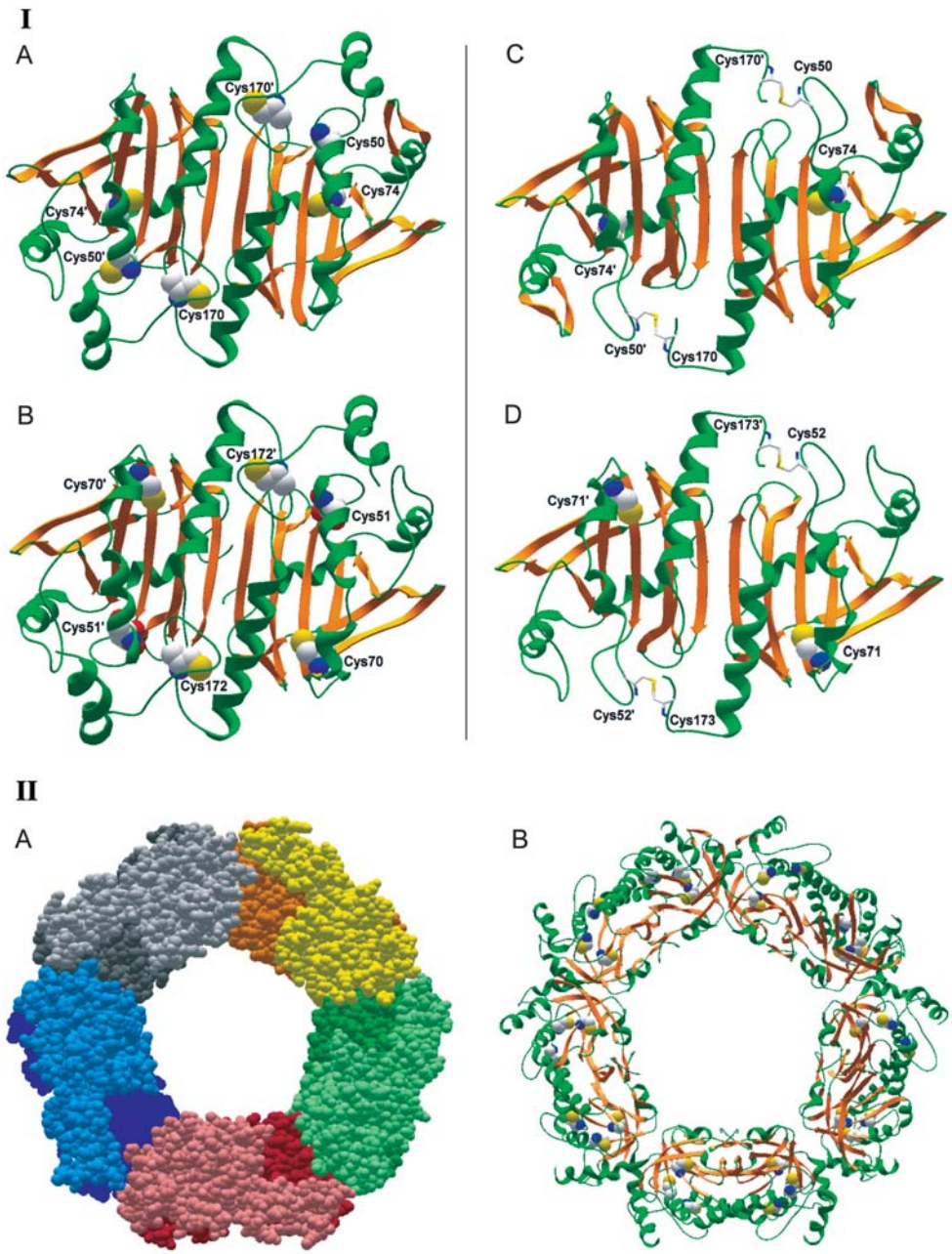

Figure 3 Models of dimeric and decameric PfTPx1.
(I) Models of reduced and oxidised dimeric PfTPx1 and comparison with the crystal structures of human PrxII and PrxI from rat. (A) Model of reduced dimeric PfTPx1. (B) Structure of the A-B dimer of human PrxII (Schröder et al., 2000), which was used as a template for (A). (C) Model of oxidised dimeric PfTPx1 with an intermolecular disulfide bond. (D) Structure of PrxI from rat (Hirotsu et al., 1999), which was used as a template for (C). All cysteine residues are highlighted to facilitate comparisons; 24 residues at the C-terminus of PrxI are not resolved in the crystal structure. The force field energies of the structures were calculated using the GROMOS96 implementation of spdbv: A, -11.64 MJ/mol; B, -12.90 MJ/mol; C, -9.76 MJ/mol; and D, -8.36 MJ/mol. (II) Model of (a2)5 decameric PfTPx1 based on the crystal structure of human PrxII (Schröder et al., 2000). (A) CPK space-filling model. Each of the 10 subunits forming a dimer is shown in a similar colour. (B) Ribbon representation of decameric PfTPx1, with all cysteine residues highlighted as CPK space-filling models.

basic criterion for catalysis with Plrx as substrate for TPx1 is fulfilled.

Among the links between nitric oxide metabolism and malaria, protein nitration in the brain of cerebral malaria patients (Clark and Schofield, 2000) is a prominent example. The nitration processes suggest a role of NO and derivatives in the pathogenesis of the disease. On the other hand, peroxynitrite seems to be a principal mediator of the antiplasmodial activity of activated macrophages (Fritsche et al., 2001). The need for RNS detoxification systems in *P. falciparum* is reinforced by the fact that the parasite digests large amounts of hemoglobin, an important scavenger of nitric oxide (Herold, 1998) and a strong promoter of oxidative processes (Deliconstaninos et al., 1996). Moreover, erythrocytes as the host cells of malarial parasites harbour high concentrations of oxygen and produce NO via the action of a Ca^{2+}-calmodulin-dependent NO synthase (Deliconstaninos et al., 1996).

Which enzymes might be involved in detoxification of RNS? Interestingly, human and *P. falciparum* glutathione reductase are inhibited by peroxynitrite, *S*-nitrosoglutathione, and dinitrosyl-dithiol-iron complexes, but also accept peroxynitrite as substrate, with K_m values of ~70 μM and k_{cat} values of 10 and 126 min^{-1} (Francescutti et al., 1996; Becker et al., 1998; Savvides et al., 2002). The approximately 13-fold higher activity of the plasmodial orthologue may underline the parasite's requirement for efficient detoxification of RNS. Peroxynitrite reductase activity has been described for Prx from various organisms, including a number of pathogens (Bryk et al., 2000; Barr and Gedamu, 2001, 2003; Peshenko and Shichi, 2001; Wong et al., 2002; Trujillo et al., 2004). In *Trypanosoma cruzi*, for example, tryparedoxin peroxidase is suggested to play an important role in peroxynitrite detoxification because of its high (9×10^5 M^{-1} s^{-1}) second-order rate constants (Thomson et al., 2003; Trujillo et al., 2004). Several authors have postulated that the peroxynitrite reductase activity can be extended to most if not all Prxs (Wong et al., 2002). Recently, as the first 2-Cys Prx of higher eukaryotes, a chloroplast 2-Cys Prx from *Arabidopsis thaliana* was demonstrated to have this activity (Sakamoto et al., 2003).

Here we have shown that PfTPx1 also possesses peroxynitrite reductase activity. At pH 7.4 and 25°C, the second-order rate constant determined was 4×10^5 M^{-1} s^{-1}. In comparison, the estimated catalytic efficiency k_{cat}/K_m for *P. falciparum* glutathione reductase is $\geq3\times10^4$ M^{-1} s^{-1} (Savvides et al., 2002). Prxs are among the most abundant proteins in *E. coli* and mammalian cells (Wood et al., 2003), suggesting that the cellular protein concentration of TPx1 – which is constitutively expressed in the parasite cytoplasm throughout the erythrocytic stages (Yano et al., 2005) – is presumably higher than the concentration of glutathione reductase. Furthermore, mRNA and protein levels of TPx1 are increased in response to exogenous oxidative stress, whereas the protein concentration of glutathione reductase does not seem to be affected (see Figure 2 in Akerman and Müller, 2003). In comparison with wild-type parasites, erythrocytic stages of PfTPx1 knock-out parasites exhibit a reduced growth rate when treated with paraquat and sodium nitroprusside, demonstrating that the enzyme is involved in protecting the parasite against oxidative and nitrosative stress (Komaki-Yasuda et al., 2003). In the absence of these compounds, however, knock-out parasites grow normally (Komaki-Yasuda et al., 2003), suggesting that PfTPx1 is not essential for the detoxification of endogenously produced ROS and/or RNS in *in vitro* cultures.

PfTPx1 possesses three cysteine residues: the peroxidatic cysteine Cys50, Cys170, which is conserved in the group of classical 2-Cys-Prxs, and Cys74, conserved in type V-Prx. To study the reaction mechanism of TPx1 in more detail, we generated and characterised two mutants of the enzyme, namely C74A and C170A (Table 2). Loss of Cys74 does not significantly influence Trx-dependent peroxidase activity of TPx1, whereas the catalytic efficiency of the C170A mutant is drastically decreased. We are aware of the fact that calculation of apparent K_m and V_{max} values is critical for peroxiredoxins, because this group of enzymes generally does not follow Michaelis-Menten kinetics and many members are rapidly inactivated by hydrogen peroxide (Hofmann et al., 2002). However, apparent K_m values have previously been successfully approximated for TPx1 – particularly under fixed concentrations of the second substrate (Rahlfs and Becker, 2001; Akerman and Müller, 2003) – and saturation kinetics were obtained. Furthermore, our kinetic values are well comparable with literature data (Akerman and Müller, 2003).

Gel electrophoresis studies and molecular modelling clearly indicate that Cys170 is the residue responsible for disulfide formation in TPx1. Presumably, the wild-type of TPx1 reacts comparably to other typical 2-Cys Prxs (Hofmann et al., 2002; Wood et al., 2003): the oxidation of Cys50 to a sulfenic acid by a hydroperoxide is followed by the formation of an intermolecular disulfide bond between Cys50 and Cys170′. Cys170′ is more accessible than Cys50, and thus it is likely that the electron donor attacks the disulfide at Sγ of Cys170′, forming an intermediate disulfide with TPx1 and releasing reduced Cys50. The catalytic cycle is completed when the second thiol of the substrate attacks the disulfide and reduced TPx1 is released. The structure models support the assumption that reaction of TPx1C170A with Trx could be explained by direct reaction of Cys50 with the electron donor. In this case, the unwinding of helix α2 (Figure 3I), carrying the peroxidatic cysteine sulfenic acid, and the formation of a disulfide bond between Cys50 and the bulky electron donor Trx have to be postulated. Furthermore, the models of reduced and oxidised TPx1 (Figure 3IA,C,II) support our experimental data *in vitro*, showing that Cys74 does not influence the catalytic mechanism: first, the residue is hardly accessible for substrates. Second, it is far away from other cysteine residues of the same or adjacent subunits.

Peroxiredoxins have been shown to exhibit characteristic oligomerisation behaviour, switching between a dimeric oxidised and a decameric reduced state (Hofmann et al., 2002; Wood et al., 2003). Association at both the monomer-monomer interface (Sarma et al., 2005) and at the interface between two dimers is probably based on hydrophobic interactions (Alphey et al., 2000). The dimer-dimer interface region II of mammalian 2-Cys Prx (Wood et al., 2003), including Thr88, is also conserved in TPx1. This (partially) explains the similar oligomerisation behaviour of TPx1 (Akerman and Müller, 2003) and mammalian 2-Cys Prx (Schröder et al., 2000; Wood et al., 2003), although the basic patch on one side of helix α3 of TPx1 differs from the human enzyme. This patch might be used to develop inhibitors to prevent oligomerisation of TPx1. Further studies will show whether TPx1 can be phosphorylated at Thr88 in analogy to mammalian 2-Cys Prx, a modification that presumably triggers decomposition and/or enzymatic activity of Prx (Wood et al., 2003). Prxs are also involved in redox regulation of metabolic processes (Hofmann et al., 2002). In oxidatively stressed erythrocytes, the decameric form of PrxII could act as a redox sensor via accumulation and association with membranes (Schröder et al., 2000), suggesting a connection between oligomerisation behaviour and redox signalling. In addition to the ROS and RNS detoxifying activity, this may also be true for PfTPx1.

We have shown that PfTPx1 is – besides thioredoxin – able to interact with plasmoredoxin and that peroxynitrite is – besides different peroxides – a substrate for the enzyme. But what is the physiological substrate? In the case of hydroperoxide, small amounts are detoxified effectively, but higher amounts lead to inactivation of the enzyme. The estimated turnover of peroxynitrite by TPx1 assuming a steady-state concentration of 20 nM for ONOOH (Valdez et al., 2000) and of 50 μM for reduced TPx1 in *P. falciparum*, is 1 μM/s. Thus, even a 50-fold excess of ONOOH could be detoxified effectively.

Materials and methods

Materials

Recombinant *P. falciparum* Trx and thioredoxin reductase (TrxR) were produced as described by Kanzok et al. (2000), and PfPlrx as described by Becker et al. (2003). Pfu polymerase was obtained from Promega (Mannheim, Germany), and restriction enzymes and dNTP were from MBI Fermentas Products (St. Leon-Rot, Germany). NADPH was purchased from BioMol (Hamburg, Germany), cystatin and pepstatin were obtained from Sigma (Steinheim, Germany), and H_2O_2 was from Merck (Frankfurt/Main, Germany). All other reagents were from Roth (Karlsruhe, Germany). The DTNB stock solution was prepared with dimethylsulfoxide (DMSO) and stored at -20°C. NADPH and H_2O_2 solutions were daily prepared in assay buffer.

Site-directed mutagenesis of TPx1

The following primers were obtained from MWG (Ebersberg, Germany) for site-directed mutagenesis: TPx1C74Af, TTGAATTAATAGGCGCTAGTGTGGATAG; TPx1C74Ar, CTATCCACACTAGCGCCT ATTAATTCAA; TPx1C170Af, GATGTTGCTCCAGCAAACTGGAAAAAG; and TPx1C170Ar, CTTTTTCCAGTTTGCTGGAGCAACATC. In volumes of 50 μl of buffer, 2 pM of each primer, 30 ng of template vector (TPx1/pQE30 generated as described by Rahlfs and Becker, 2001) were mixed and 3 U of Pfu polymerase were added after the initial denaturation step of 3 min at 95°C. Then 25 cycles consisting of 95°C for 30 s, 60°C for 30 s and 72°C for 10 min were carried out, followed by a final elongation step of 5 min at 72°C. Purified and DpnI-restricted PCR products (mutated vectors) were transformed into *E. coli* strain XL1Blue and, after checking the sequence, into *E. coli* M15 cells for heterologous expression.

Expression and purification of TPx1 wild-type and mutants

Expression and purification were carried out as described by Rahlfs and Becker (2001) with slight modifications. Purification was always carried out in parallel with the different enzyme forms under reducing conditions to avoid precipitation. Proteins were eluted with $\geq$75 mM imidazole and taken up in 10 mM dithiothreitol. Purity was demonstrated by 15% SDS-PAGE. After concentration via ultrafiltration and dialysis (directly before use), protein concentration was determined using the calculated extinction coefficients (ε_{280} 22.0 and 21.9 mM^{-1} cm^{-1} for the wild type and mutants, respectively) and the Bradford protein dye assay. Theoretical molecular masses are 23 206 Da (wild type) and 23 174 Da (mutants). Protein yields were 15–25 mg/l cell culture.

Enzyme activity of the mutants compared with the wild type

Assays were performed in 100 mM Tris/HCl, 1 mM EDTA, pH 8.0, at 37°C in a final volume of 0.4 ml. NADPH (0.2 mM) was mixed with TrxR (0.1 U/ml), varying concentrations of Trx1, and TPx1 (0.25 μM of wild type and the C74A mutant, and 10 μM of the C170A mutant). After monitoring the baseline for 3 min, assays were started by the addition of 0.1 mM H_2O_2. Activity was determined by following the decrease in absorbance at 340 nm, representing the consumption of NADPH. Due to the rapid inactivation of TPx1 by H_2O_2, only the first 20 s of the reaction were taken into account. Absorbance decreases were corrected for the Trx1-dependent H_2O_2 reduction.

Reduction of TPx1 by plasmoredoxin

Purified plasmoredoxin (approx. 50 μM) was incubated in 50 mM $NaPO_4$ buffer, 300 mM NaCl (pH 8.0) with 2 mM dithiothreitol for 30 min to quantitatively reduce the four cysteine residues of the protein. After dilution of the sample, excess dithiothreitol was removed by Ni-NTA (nickel-nitrilotriacetic acid) agarose chromatography. Various incubation mixtures were prepared in 100 mM sodium phosphate, 1 mM EDTA, pH 7.4 (see Table 1). Concentrations of Plrx, TPx1, and H_2O_2 were 100, 80 and 200 μM, respectively. Aliquots (40 μl) of the incubation mixtures were taken immediately and after 15 min, then diluted to a final assay volume of 400 μl, yielding assay concentrations of 10 μM for Plrx and 8 μM for TPx1. DTNB (assay concentration of 400 μM) was added and the generation of 5-thio-2-nitrobenzoate was detected at 412 nm (ε=13.6 mM^{-1} cm^{-1}), allowing quantitative determination of sulfhydryl groups present in the assay mixture. In a parallel experiment, Trx1 was used instead of Plrx as a positive control.

Peroxynitrite synthesis

Peroxynitrite was synthesised in a quenched-flow reactor as described previously (Radi et al., 1991a), and excess hydrogen peroxide was removed by treatment with MnO_2. Peroxynitrite concentration was determined spectrophotometrically by the measurement of absorbance at 302 nm in 1 M NaOH (ε_{302}=1670 M^{-1} cm^{-1}).

TPx1-induced peroxynitrite decomposition

To reduce TPx1 thiols, the enzyme was treated overnight with 10 mM dithiothreitol at 4°C. Excess reductant was removed immediately before use by gel filtration on Hitrap columns (Amersham) using degassed 100 mM sodium phosphate buffer plus 0.1 mM DTPA, pH 7 as eluent, followed by extensive bubbling with argon.

The kinetics of peroxynitrite reaction with reduced TPx1 was studied in a stopped-flow spectrophotometer (SX-17MV; Applied Photophysics, Leatherhead, UK) with a mixing time of less than 2 ms, following initial rates of peroxynitrite decomposition at 302 nm in the presence of different enzyme concentrations in 50 mM sodium phosphate buffer, 0.1 mM DTPA, pH 7.4 at 37°C (or 25°C). To ensure the accuracy of the rate constant determinations, 200 absorbance measurements were acquired during the initial part of the reaction (first 20 ms).

TPx1 structure prediction

Models of oxidised and reduced TPx1 are based on the crystal structures of decameric human PrxII (Schröder et al., 2000) and dimeric PrxI (Hirotsu et al., 1999) from rat (Protein Data Bank accession numbers 1QMV and 1QQ2). Alignments of TPx1 and Prxs were optimised manually in the Swiss-PDB Viewer (spdbv).

Computations of the models were carried out at the Swiss-Model server using the optimise (project) mode (Guex and Peitsch, 1997; Schwede et al., 2003). The force field energy of the models was calculated with the GROMOS96 implementation of spdbv.

Acknowledgements

The authors wish to thank Marina Fischer and Elisabeth Fischer for their excellent technical assistance and Professor Leopold Flohé (Magdeburg) for logistic support. The study was funded by the Deutsche Forschungsgemeinschaft (SFB 535, TP A12 to K.B.). R.R. was supported by a grant from the Howard Hughes Medical Institute, USA.

References

Akerman, S.E. and Müller, S. (2003). 2-Cys peroxiredoxin PfTrx-Px1 is involved in the antioxidant defence of *Plasmodium falciparum*. Mol. Biochem. Parasitol. *130*, 75–81.

Alphey, M.S., Bond, C.S., Tetaud, E., Fairlamb, A.H., and Hunter, W.N. (2000). The structure of reduced tryparedoxin peroxidase reveals a decamer and insight into reactivity of 2-Cys-peroxiredoxins. J. Mol. Biol. *300*, 903–916.

Arteel, G.E., Briviba, K., and Sies, H. (1999). Protection against peroxynitrite. FEBS Lett. *445*, 226–230.

Barr, S.D. and Gedamu, L. (2001). Cloning and characterisation of three differentially expressed peroxidoxin genes from *Leishmania chagasi*. Evidence for an enzymatic detoxification of hydroxyl radicals. J. Biol. Chem. *276*, 34279–34287.

Barr, S.D. and Gedamu, L. (2003). Role of peroxidoxins in *Leishmania chagasi* survival. Evidence of an enzymatic defense against nitrosative stress. J. Biol. Chem. *278*, 10816–10823.

Becker, K., Savvides, S.N., Keese, M., Schirmer, R.H., and Karplus, P.A. (1998). Enzyme inactivation through sulfhydryl oxidation by physiologic NO-carriers. Nat. Struct. Biol. *5*, 267–271.

Becker, K., Kanzok, S.M., Iozef, R., Fischer, M., Schirmer, R.H., and Rahlfs, S. (2003). Plasmoredoxin, a novel redox-active protein unique for malarial parasites. Eur. J. Biochem. *270*, 1057–1064.

Becker, K., Tilley, L., Vennerstrom, J.L., Roberts, D., Rogerson, S., and Ginsburg, H. (2004). Oxidative stress in malaria parasite-infected erythrocytes: host-parasite interactions. Int. J. Parasitol. *34*, 163–189.

Bryk, R., Griffin, P., and Nathan, C. (2000). Peroxynitrite reductase activity of bacterial peroxiredoxins. Nature *407*, 211–215.

Clark, I.A. and Schofield, L. (2000). Pathogenesis of malaria. Parasitol. Today *16*, 451–454.

Deliconstantinos, G., Villiotou, V., and Stravrides, J.C. (1996). Tumour promoter *tert*-butyl-hydroperoxide induces peroxynitrite formation in human erythrocytes. Anticancer Res. *16*, 2969–2979.

Denicola, A., Souza, J.M., and Radi, R. (1998). Diffusion of peroxynitrite across erythrocyte membranes. Proc. Natl. Acad. Sci. USA *95*, 3566–3571.

Deponte, M. and Becker, K. (2005). Biochemical characterization of *Toxoplasma gondii* 1-Cys peroxiredoxin 2 with mechanistic similarities to typical 2-Cys Prx. Mol. Biochem. Parasitol. *140*, 87–96.

Deponte, M., Becker, K., and Rahlfs, S. (2005). *Plasmodium falciparum* glutaredoxin-like proteins. Biol. Chem. *386*, 33–40.

Douki, T., Cadet, J., and Ames, B.N. (1996). An adduct between peroxynitrite and 2′-deoxyguanosine: 4,5-dihydro-5-hydroxy-4-(nitrosooxy)-2′-deoxyguanosine. Chem. Res. Toxicol. *9*, 3–7.

Estevez, A.G., Crow, J.P., Sampson, J.B., Reiter, C., Zhuang, Y., Richardson, G.J., Tarpey, M.M., Barbeito, L., and Beckman, J.S. (1999). Induction of nitric oxide-dependent apoptosis in motor neurons by zinc-deficient superoxide dismutase. Science *286*, 2498–2500.

Francescutti, D., Baldwin, J., Lee, L., and Mutus, B. (1996). Peroxynitrite modification of glutathione reductase: modeling studies and kinetic evidence suggest the modification of tyrosines at the glutathione disulfide binding site. Protein Eng. *9*, 189–194.

Fritsche, G., Larcher, C., Schennach, H., and Weiss, G. (2001). Regulatory interactions between iron and nitric oxide metabolism for immune defense against *Plasmodium falciparum* infection. J. Infect. Dis. *183*, 1388–1394.

Gamain, B., Langsley, G., Fourmaux, M.N., Touzel, J.P., Camus, D., Dive, D., and Slomianny, C. (1996). Molecular characterization of the glutathione peroxidase gene of the human malaria parasite *Plasmodium falciparum*. Mol. Biochem. Parasitol. *78*, 237–248.

Guex, N. and Peitsch, M.C. (1997). SWISS-MODEL and the Swiss-PdbViewer: an environment for comparative protein modeling. Electrophoresis *18*, 2714–2723.

Herold, S. (1998). Kinetic and spectroscopic characterization of an intermediate peroxynitrite complex in the nitrogen monoxide induced oxidation of oxyhemoglobin. FEBS Lett. *439*, 85–88.

Hirotsu, S., Abe, Y., Okada, K., Nagahara, N., Hori, H., Nishino, T., and Hakoshima, T. (1999). Crystal structure of a multifunctional 2-Cys peroxiredoxin heme-binding protein 23 kDa/proliferation-associated gene product. Proc. Natl. Acad. Sci. USA *96*, 12333–12338.

Hofmann, B., Hecht, H.-J., and Flohé, L. (2002). Peroxiredoxins. Biol. Chem. *383*, 347–364.

Ischiropoulos, H. (2003). Oxidative modifications of alpha-synuclein. Ann. N.Y. Acad. Sci. *991*, 93–100.

Kanzok, S.M., Fechner, A., Bauer, H., Ulschmid, J.K., Muller, H.M., Botella-Munoz, J., Schneuwly, S., Schirmer, R.H., and Becker, K. (2001). Substitution of the thioredoxin system for glutathione reductase in *Drosophila melanogaster*. Science *291*, 643–646.

Kanzok, S.M., Schirmer, R.H., Turbachova, I., Iozef, R., and Becker, K. (2000). The thioredoxin system of the malaria parasite *Plasmodium falciparum*. Glutathione reduction revisited. J. Biol. Chem. *275*, 40180–40186.

Kawazu, S., Tsuji, N., Toshimitsu H., Kawai, S., Matsumoto, Y., and Kano, S. (2000). Molecular cloning and characterization of a peroxiredoxin from the human malaria parasite *Plasmodium falciparum*. Mol. Biochem. Parasitol. *109*, 165–169.

Kawazu, S., Ikenoue, N., Takemae, H., Komaki-Yasuda, K., and Kano, S. (2005). Roles of 1-Cys peroxiredoxin in haem detoxification in the human malaria parasite *Plasmodium falciparum*. FEBS J. *272*, 1784–1791.

Komaki-Yasuda, K., Kawazu, S., and Kano, S. (2003). Disruption of the *Plasmodium falciparum* 2-Cys peroxiredoxin gene renders parasites hypersensitive to reactive oxygen and nitrogen species. FEBS Lett. *547*, 140–144.

Konorev, E.A., Hogg, N., and Kalyanaraman, B. (1998). Rapid and irreversible inhibition of creatine kinase by peroxynitrite. FEBS Lett. *427*, 171–174.

Krauth-Siegel, R.L., Bauer, H., and Schirmer, R.H. (2005). Dithiol proteins as guardians of the intracellular redox milieu in parasites: old and new drug targets in trypanosomes and malaria-causing plasmodia. Angew. Chem. Int. Ed. *44*, 690–715.

Krnajski, Z., Walter, R.D., and Müller, S. (2001). Isolation and functional analysis of two thioredoxin peroxidases (peroxiredoxins) from *Plasmodium falciparum*. Mol. Biochem. Parasitol. *113*, 303–308.

Pedrajas, J.R., Miranda-Vizuete, A., Javanmardy, N., Gustafsson, J.A., and Spyrou, G. (2000). Mitochondria of *Saccharomyces cerevisiae* contain one-conserved cysteine type peroxiredoxin with thioredoxin peroxidase activity. J. Biol. Chem. *275*, 16296–16301.

Peshenko, I.V. and Shichi, H. (2001). Oxidation of active center cysteine of bovine 1-Cys peroxiredoxin to the cysteine sulfenic acid form by peroxide and peroxynitrite. Free Radic. Biol. Med. *31*, 292–303.

Quijano, C., Alvarez, B., Gatti, R.M., Augusto, O., and Radi, R. (1997). Pathways of peroxynitrite oxidation of thiol groups. Biochem. J. *322*, 167–173.

Radi, R., Beckman, J.S., Bush, K.M., and Freeman, B.A. (1991a). Peroxynitrite-induced membrane lipid peroxidation: the cytotoxic potential of superoxide and nitric oxide. Arch. Biochem. Biophys. *288*, 481–487.

Radi, R., Beckman, J.S., Bush, K.M., and Freeman, B.A. (1991b). Peroxynitrite oxidation of sulfhydryls. The cytotoxic potential of superoxide and nitric oxide. J. Biol. Chem. *266*, 4244–4250.

Radi, R., Denicola, A., Alvarez, B., Ferrer-Sueta, G., and Rubbo, H. (2000). The biological chemistry of peroxynitrite. In: Nitric Oxide. Biology and Pathobiology, L. Ignarro, ed. (San Diego, USA: Academic Press), pp. 57–82.

Rahlfs, S. and Becker, K. (2001). Thioredoxin peroxidases of the malarial parasite *Plasmodium falciparum*. Eur. J. Biochem. *268*, 1404–1409.

Rahlfs, S., Schirmer, R.H., and Becker, K. (2002). The thioredoxin system of *Plasmodium falciparum* and other parasites. Cell. Mol. Life Sci. *59*, 1024–1041.

Rahlfs, S., Nickel, C., Deponte, M., Schirmer, R.H., and Becker, K. (2003). *Plasmodium falciparum* thioredoxins and glutaredoxins as central players in redox metabolism. Redox Rep. *8*, 246–250.

Sakamoto, A., Tsukamoto, S., Yamamoto, H., Ueda-Hashimoto, M., Takahashi, M., Suzuki, H., and Morikawa, H. (2003). Functional complementation in yeast reveals a protective role of chloroplast 2-Cys peroxiredoxin against reactive nitrogen species. Plant J. *33*, 841–851.

Sarma, G.N., Nickel, C., Rahlfs, S., Fischer, M., Becker, K., and Karplus, P.A. (2005). Crystal structure of a novel *Plasmodium falciparum* 1-Cys peroxiredoxin. J. Mol. Biol. *346*, 1021–1034.

Savvides, S.N., Scheiwein, M., Böhme, C.C., Arteel, G.E., Karplus, P.A., Becker, K., and Schirmer, R.H. (2002). Crystal structure of the antioxidant enzyme glutathione reductase inactivated by peroxynitrite. J. Biol. Chem. *277*, 2779–2784.

Schröder, E., Littlechild, J.A., Lebedev, A.A., Errington, N., Vagin, A.A., and Isupov, M.N. (2000). Crystal structure of decameric 2-Cys peroxiredoxin from human erythrocytes at 1.7 Å resolution. Structure Fold Des. *8*, 605–615.

Schwede, T., Kopp, J., Guex, N., and Peitsch, M.C. (2003). SWISS-MODEL: an automated protein homology-modeling server. Nucleic Acids Res. *31*, 3381–3385.

Skinner, K.A., White, C.R., Patel, R., Tan, S., Barnes, S., Kirk, M., Darley-Usmar, V., and Parks, D.A. (1998). Nitrosation of uric acid by peroxynitrite. Formation of a vasoactive nitric oxide donor. J. Biol. Chem. *273*, 24491–24497.

Souza, J.M. and Radi, R. (1998). Glyceraldehyde-3-phosphate dehydrogenase inactivation by peroxynitrite. Arch. Biochem. Biophys. *360*, 187–194.

Sztajer, H., Gamain, B., Aumann, K.D., Slomianny, C., Becker, K., Brigelius-Flohe, R., and Flohe, L. (2001). The putative glutathione peroxidase gene of *Plasmodium falciparum* codes for a thioredoxin peroxidase. J. Biol. Chem. *276*, 7397–7403.

Thomson, L., Denicola, A., and Radi, R. (2003). The trypanothione-thiol system in *Trypanosoma cruzi* as a key antioxidant mechanism against peroxynitrite-mediated cytotoxicity. Arch. Biochem. Biophys. *412*, 55–64.

Trujillo, M. and Radi, R. (2002). Peroxynitrite reaction with the reduced and the oxidized forms of lipoic acid: new insights into the reaction of peroxynitrite with thiols. Arch. Biochem. Biophys. *397*, 91–98.

Trujillo, M., Budde, H., Pineyro, M.D., Stehr, M., Robello, C., Flohe, L., and Radi, R. (2004). *Trypanosoma brucei* and *Trypanosoma cruzi* tryparedoxin peroxidases catalytically detoxify peroxynitrite via oxidation of fast reacting thiols. J. Biol. Chem. *279*, 34175–34182.

Valdez, L.B., Lores Arnaiz, S., Bustamante, J., Alvarez, S., Costa, L.E., and Boveris, A. (2000). Free radical chemistry in biological systems. Biol. Res. *33*, 65–70.

Wong, C.-M., Zhou, Y., Ng, R.W.M., Kung, H., and Jin, D.-Y. (2002). Cooperation of yeast peroxiredoxins Tsa1p and Tsa2p in the cellular defense against oxidative and nitrosative stress. J. Biol. Chem. *277*, 5385–5394.

Wood, Z.A., Schröder E., Robin Harris, J., and Poole, L.B. (2003). Structure, mechanism and regulation of peroxiredoxins. Trends Biochem. Sci. *28*, 32–40.

Yano, K., Komaki-Yasuda, K., Kobayashi, T., Takemae, H., Kita, K., Kano, S., and Kawazu, S. (2005). Expression of mRNAs and proteins for peroxiredoxins in *Plasmodium falciparum* erythrocytic stage. Parasitol. Int. *54*, 35–41.

Received July 21, 2005; accepted August 9, 2005